Solidification of binary aqueous solution cooled from above

Solidification of Binary Aqueous Solution Cooled from Above

Shigeo Kimura*, Yohei Nohara**, Takahiro Kiwata***, and Nobuyoshi Komatsu***

* Institute of Nature and Environmental Technology, Kanazawa University, Japan

** Honda Motor Co., Ltd., Japan

*** School of Mechanical Engineering, Kanazawa University, Japan

Abstract

Freezing and melting phenomena are important in many different fields, including crystal growth, casting, metallurgy, geophysics and oceanography. Solidification from multi-component solution is the one often observed in nature. In order to investigate basic features of freezing processes of binary systems, we conducted a series of laboratory experiments in a rectangular box cooled from above using aqueous $NaNO_3$ solution. During the freezing, the solid phase always grows into many needle-like crystals called mushy layer. We measured the growth of the mushy layer thickness, the solid fraction, the temperature and the concentration distributions. The average solid fraction is found to increase with time in the mushy layer. This causes a slow descent of the released solute in the mushy layer and its eventual fall into the liquid region below because of gravity. We propose a one-dimensional model to explain the horizontally-averaged mushy layer growth. In the model, the estimate of a heat flux at the mushy-liquid interface due to natural convection is found essential for

a correct prediction. The proposed theory predicts well the growth of the mushy-layer and the average solid fraction, once the convective heat flux is properly given.

Key words: Solidification, Natural Convection, Heat Transfer, Binary Solution, Double Diffusion, Mushy Layer

1. Introduction

Solidification and melting can be observed in a wide range of spectrum from water freezing in our daily life to large scale geophysical problems, such as sea ice formation in the arctic region, solidification in magma chambers, evolution of crustal structures in planetary interiors[1]. In the field of engineering, it is equally common in such processes as casting in metallurgy and silicon wafer production in semiconductor industry. The latter is particularly concerned with the influence of convection on the product quality. Therefore, in the semiconductor industry it is imperative to establish a mean to control the strength of convection during the solidification from molten silicon[2]. In the bio-medical engineering, non-equilibrium solidification during the freezing processes of living cells has been also investigated[3].

Both in the geo-heat pump system that intends to make use of low enthalpy thermal energy in aquifer systems, and in the heat extraction from deep magma chambers, ice or solid phase formed around the ground heat exchanger significantly increases the thermal resistance, and thereby reduces the heat transfer performance. Therefore, it is important to establish a way for controlling the size of the solid phase by modulating the surface temperature of the heat exchanger[4]. The solid phase response

in a water-saturated porous medium has been studied when the cooling surface temperature is varied periodically[5].

There are many cases, where the liquid phase consists of more than one component. For example, the ice formation and melting in the arctic sea, which is often taken as an indicator of global warming, is a typical example[6]. Molten magma is also a typical multi-component system, in which molten silica, as a major component, dissolves many different kinds of metals and minerals. Since the solidifying process in a multi-component system depends not only on the temperature, but also on the concentration of solvent, the prediction and analysis becomes much harder than that for a single component system.

One of the typical two-component systems, which are suited for laboratory experiments, is an aqueous solution of ammonium chloride. Many experimental works using the ammonium chloride solution have been reported up to today[7-12]. Numerical solutions on solidifying two-component aqueous solution have been conducted by Beckermann and Viskanta[12], and Thompson and Szekely[14]. However, their numerical predictions do not completely agree with the experimental results.

On the other hand, one dimensional analysis of solidification process has many advantages for its simplicity. For example, the mathematical formulation is much easier, and the model deals with lesser number of parameters, and the results are easy to understand intuitively. A one-dimensional model often helps providing useful information for understanding seemingly complex processes, such as solidification in multi-component systems. Huppert et al.[15,16] performed a laboratory experiment of magma solidification, employing aqueous isopropanol solution, and a one-dimensional analysis was proposed. The experiment was carried out in an adiabatic box cooled from above, and it was found that convection had a significant effect on the solidification.

They also demonstrated that the one-dimensional analysis was able to explain the most of the features observed in the experiment.

In this work, we carry out solidification experiments in a box cooled from above and heated on the bottom, and with adiabatic side walls, using aqueous sodium-nitrite solution, whose liquidus has a mild slope in the phase diagram, and allows us a wide range of freedom to set up initial concentration conditions. Four different combinations of initial concentrations and cooling temperatures have been investigated, and the time-evolution of the mushy layer, the solid fraction, the temperature, and the concentration have been monitored in the course of the experiment. A one-dimensional analytical model is also proposed in order to explain the experimental observations.

Nomenclature

C : concentration wt%

c_p : specific heat at constant pressure, $\mathrm{kJ/(kg \cdot K)}$

D : characteristic length scale of dendrite

f : solid layer thickness, m

h: convective heat transfer coefficient, $\mathrm{W/(m^2 \cdot K)}$

H: height of rectangular vessel, m

k: thermal conductivity, $\mathrm{W/(m \cdot K)}$

K: permeability of mushy layer, $\mathrm{m^2}$

L: latent heat, kJ/kg

m: slope of the liquidus in phase diagram

q'': heat flux, $\mathrm{W/m^2}$

t: time, s

T: temperature, ℃

V: vessel volume, m^3

α: thermal diffusivity, m^2/s

β: thermal expansion coefficient, K^{-1}

γ: exponent

η: similarity variable

θ: nondimensional temperature

λ: root of transcendental equation

ν: kinematic viscosity, m^2/s

ρ: density, kg/m^3

ϕ: average solid fraction

Subscripts and Superscripts

c: cooled surface

C: solvent concentration

f: solid-liquid boundary

h: heated surface

l: liquid phase

L: liquidus

m: mushy region

s: solid phase

o: initial state

2. Experimental Apparatus and Measurement

2.1 Experimental Apparatus

Figure 1 shows a schematic diagram of an experimental apparatus and a measurement system. Figure 2 shows a detailed sketch of a rectangular vessel, in which a solid layer grows from a binary aqueous solution. The vessel has inner dimensions of 180mm in width, 175mm in depth, and 180mm in height. The vessel's side walls are constructed with 15mm thick acrylic plates, and the top and the bottom are made of copper plates in order to ensure the respective uniform temperatures. The entire vessel is placed in another slightly larger vessel of a similar shape for preventing the undesirable heat penetration from the environment. A Peltier cooling unit is also installed to maintain the temperature of the air gap between the vessels, at a value equal to the average of the top and the bottom temperatures. Furthermore, the whole system, except cooling units, is kept in the temperature controlled room at $5\,^{\circ}\mathrm{C}$ during the experiment.

The top and bottom copper plates have grooved channels, through which two brines (ethylene glycol aqueous solution) at respective temperatures are running, so that each plate is maintained at a desired temperature. The top plate is cooled to sub zero temperatures below the liquidus line, and the solid phase starts growing there. On the other hand, the bottom plate is always kept at $0\,^{\circ}\mathrm{C}$, which is above the liquidus line. Therefore, even at the steady state, the lower half is occupied by liquid phase. A small tube attached on the lower side wall allows releasing the excess volume of aqueous solution, due to the volume expansion by ice formation in the vessel, which is led to a pipette and used to measure the solid fraction within the vessel.

All-together 20 T-type thermocouples are installed in the top and bottom plates, as well as in the vertical positions adjacent to the side wall. In order to measure the

respective surface temperatures of the copper plate, a small hole is drilled from the back to 1mm position from the surface in each plate, and a thermocouple is glued in the hole. The vertically placed thermocouples are positioned closely to each other near the top and the bottom, where the sharp thermal boundary layers are expected. In the opposite side wall, a long vertical slit is made, and it was plugged with silicon rubber, through which a micro-syringe is inserted to extract a small amount of liquid and to determine the sodium nitrite concentration at an arbitrary vertical position.

*[**Figure 1**]*

*[**Figure 2**]*

2.2 Measurement

The initial condition is established by administering 0°C brine into the top and bottom copper plates, and leaving the system until the thermal equilibrium is reached. The experiment is then initiated by switching 0°C brine of the top plate to a sub -liquidus temperature, while the bottom brine is kept running at 0°C.

The solid layer thickness developed from the top is measured by taking photos from one of the transparent side walls at fixed time intervals. A scale is attached on the wall, to be used as a reference length scale. The average solid layer thickness is calculated by measuring ten local thicknesses. In the course of the experiment, it has been found that the solid-liquid boundary is not distorted significantly in the third dimension. The time evolution of the vertical temperature profile in the vessel is monitored by thermocouples. The corresponding concentration profile is obtained by extracted small amount of liquid solution (0.05ml) with the micro-syringe. The concentration was determined by measuring a refractive index of the sampled droplet.

When a binary solution, such as aqueous sodium-nitrite solution, is cooled below the liquidus temperature, a mushy layer grows on the cooling surface. The mushy layer consists of many dendrites that form a porous matrix structure. The volume of dendrite ice is determined by measuring the expelled liquid volume with the pipette. The space-averaged solid fraction of the mushy layer is then calculated by dividing the dendrite volume with the mushy layer volume.

3. Phase Diagram and Experimental Conditions

Figure 3 shows a partial phase diagram of aqueous sodium nitrite solution[16]. The eutectic temperature and concentration are -17.5 °C, and 38.5% respectively. When the solution is cooled to the liquidus temperature, ice starts forming. This phase change transforms the immediately-neighboring solution to a solute-richer state than the one at the original state, which shifts the solidification temperature to a lower value. If the expelled solute diffuses thoroughly, the solid-liquid interface condition can be predicted with the liquidus line in the phase diagram. In the present work, we have investigated four different cases, combining two different initial concentrations; 5% and 10%, and two different cooling temperatures; -6 °C and -8 °C. The experimental conditions are indicated on the phase diagram, with C_0; initial concentration, T_c; cooling temperature, and T_h; the bottom temperature, in figure 3.

*[**Figure 3**]*

4. Solid Fraction

The solid fraction of the mushy layer has been calculated based on the mass conservation law. In order to perform the calculation, it is necessary to have precise data on the densities of ice and solution at different concentrations. However, the density data of aqueous solutions at subzero temperatures are extremely scarce. Therefore, we have decided to use an approximate formula to predict the solution density at subzero temperatures. It is well known that the density extremum takes place at a certain temperature for a fixed concentration[17]. Therefore, the density extremum temperature will be a function of only the concentration[18]. Based on the Brewster-Gebhart's formula for sea water[17], we have developed a simple equation to compute the density extremum temperature as a function of concentration,

$$T_{\max} = 4.0293\left(1 - 0.5266C\right). \tag{1}$$

The density variation is approximated with a parabolic function of temperature. The two coefficients appear as functions of concentration,

$$\rho_l = a\left(T - T_{\max}\right)^2 + b, \tag{2}$$

where

$$a = -6.5335\times10^{-6} + 1.4099\times10^{-6}C - 1.6245e\times10^{-8}C^2$$

$$b = 0.99962 + 0.0073416C + 2.3206\times10^{-5}C^2 + 4.3847\times10^{-8}C^3$$

The densities predicted by equation (2) agree with the readings from Huppert-Worster's phase diagram[16] within 0.5%, in the ranges of $-8 \le T \le 0$[°C], and $0 \le C \le 20$ [wt%]. When ice is formed in the vessel, and the volume expands by ΔV, the mass conservation law requires the following relation,

$$\left[\frac{H-f}{H}\rho_l + \frac{f}{H}\left\{\phi\rho_s + \left(1-\phi\right)\rho_m\right\}\right]\left(V + \Delta V\right) = \rho_0 V. \tag{3}$$

Solving the above equation for the solid fraction ϕ, we have the next equation,

$$\phi = \frac{H\left\{\rho_0\left(V/(V+\Delta V)\right)-\rho_l\left(1-f/H\right)\right\}-\rho_m f(t)}{f(t)(\rho_s-\rho_m)}. \quad (4)$$

In the course of calculating the volume change of the aqueous solution, the expansion and contraction of the container itself due to the temperature change are also taken into considered.

5. One-dimensional Analysis

A one-dimensional analysis on solidification of binary solution was performed by Huppert-Worster[16] for neglecting natural convection in the liquid solution. In the present work, it is expected that the cooling from above causes vigorous convection in the liquid layer due to a double diffusive process. Therefore, we formulate a one-dimensional solidification model, cooperating with the convective heat transfer from the liquid layer. Figure 4 illustrates the physical model and the coordinate system.

The two basic assumptions are made in order to formulate the model.

1. A mushy layer is considered as a mixture of solid and liquid phases, and physical properties are computed as a volume averaged value.

$$\alpha_m = \phi\,\alpha_s + (1-\phi)\alpha_l \quad (5)$$

$$c_{pm} = \phi\,c_{ps} + (1-\phi)c_{pl} \quad (6)$$

$$k_m = \phi\,k_s + (1-\phi)k_l \quad (7)$$

2. The liquidus curve can be approximated linearly.

$$T = -m_L C_L \quad (8)$$

The conservation laws and the boundary conditions are expressed as follows.

(a) The energy conservation in the mushy layer;

$$\frac{\partial T}{\partial t} = \alpha_m \frac{\partial^2 T}{\partial z^2} \tag{9}$$

(b) The conservation of solute;

The solute expelled in the process of solidification will partially remain in the mushy zone, and the rest will descend into the liquid layer. Therefore the amount of solute in the mushy zone is calculated by

$$(1-\phi)\int_0^{f(t)} C_L(T)dz = \frac{(1-\phi)}{-m_L}\int_0^{f(t)} Tdz = f(t)C_m(t)\,. \tag{10}$$

The initial amount of solute must be preserved in the vessel,

$$C_0 H = C_m(t)\,f(t) + C_l(t)\big(H - f(t)\big)\,. \tag{11}$$

(c) Heat balance on the mushy-liquid boundary;

The advancement of the mushy front is governed by the difference between the conductive cooling in the mushy layer and the convective heating from the liquid layer,

$$\rho_s \phi L \frac{df}{dt} = k_s \left.\frac{\partial T}{\partial z}\right|_{f-} - h(T_h - T_f)\,. \tag{12}$$

The vertical position of the mushy front $f(t)$ is expressed by a nondimensional length scale λ,

$$f = 2\lambda\sqrt{\alpha_m t}\,. \tag{13}$$

Substituting the similarity variable $\eta = z/2\sqrt{\alpha_m t}$ and equation (13) in equation (9), the temperature in the mushy layer will be obtained as below;

$$T = T_c + (T_f - T_c)\frac{erf\,\eta}{erf\,\lambda}\,. \tag{14}$$

In the present experiments, the condition of $\eta, \lambda \ll 1$ is always satisfied, and the error function can be approximated by a linear function as $erfx \cong x$. Therefore, by

substituting the approximate expression of equation (14) in equations (10) and (11), we can obtain the average solid fraction in the mushy layer,

$$\phi(t) = 1 + \frac{2m_L \left\{ C_0 H - C_l(t)\left(H - f(t)\right)\right\}}{f(t)\left(T_f + T_c\right)}. \tag{15}$$

By employing equations (13)-(15), equation (12) can be transformed to the following transcendental equation,

$$\frac{e^{-\lambda^2}}{erf\,\lambda} = \frac{\rho_s \phi L \sqrt{\pi}\lambda}{\alpha_m k_m (T_f - T_c)} + \frac{h(T_h - T_f)\sqrt{\pi \alpha_m t}}{k_m (T_f - T_c)}. \tag{16}$$

The above equation must be solved numerically for the unknown length scale of λ for an arbitrary time *t*. Once the value of λ is obtained, equation (13) will give the vertical position of the mushy layer front. The computed results will be discussed together with the experimental data in chapter 7.

*[**Figure 4**]*

6. Convective Heat Transfer from the Liquid Layer

When the container of binary solution is cooled from above, the mushy layer will grow from the upper cooling plate. The solute expelled from ice will descend in the lower aqueous solution, and will be stirred by vigorous thermal convection to form the vertically uniform concentration profile. If the solute concentration does not give any significant effect on the thermal convection ensuing in the liquid layer, the convective heat transfer coefficient will be evaluated by Rayleigh-Nusselt correlation.

$$Ra = \frac{g\beta \Delta T (H - f)^3}{\alpha \nu} \tag{17}$$

$$Nu = ARa^{\gamma} \tag{18}$$

where $A = 0.13$, $\gamma = 1/3$ for $37000 < Ra < 10^8$ in equation (18)[19]. Both the computed and the experimentally measured convective heat transfer rates on the mushy front at steady state are listed in Table 1 for four different experimental conditions. In evaluating the experimental heat transfer rates, we assume that the steady state temperatures are always linear in the mushy layer.

It is obvious that the computed heat transfer rates are always two to five times larger than those measured by experiments. As it will be discussed in the later chapter, the solute expelled in the aqueous solution was not stirred completely in the present experiments, and it was accumulated on the bottom plate, which formed a density-stratified layer over the bottom plate. It is likely that this stably-stratified layer hampered the convective heat transfer rates. Therefore, it is not possible to estimate correctly the convection heat transfer rate by equation (18).

Another possibility to detect the bottom-to-top heat transfer rate is to measure the temperature gradients on the bottom plate, where thermocouples are positioned closely to each other, and the vertical temperature gradient can be measured precisely. The heat transfer coefficients will be then obtained by the following equations,

$$\left|q''\right| = k\left.\frac{dT}{dz}\right|_{z=H} = h(T_h - T_f)\,, \tag{19}$$

$$h = \frac{k}{T_h - T_f}\left.\frac{dT}{dz}\right|_{z=H}\,. \tag{20}$$

The heat transfer rates from bottom to top at respective steady states can be calculated using the heat transfer coefficients of equation (20). It turns out that the heat transfer rates calculated by this method agree with those derived by linear temperature assumption in the mushy layer, within 10% error. The average heat transfer coefficient

appearing in equation (16) is taken from the experimentally obtained values, as shown in Table 1, at the respective steady states, and kept it constant in equation (16) for different values of *t*.

[Table 1]

7. Experimental Results

The experimental results are shown in figures 5 - 8. Figure 5 indicates the growth of the mushy layer thickness with the time. When the initial concentration is 10wt% (experimental conditions No.3 and No.4), the mushy layer thicknesses at steady state are smaller than those of 5wt% (experimental conditions No.1 and No.2). This is due to the fact that the higher solute concentration lowers the liquidus temperature. The agreement with equation (13) is extremely good.

Figure 6 shows the time evolution of a space-averaged solid fraction. As time progresses, the temperature at a fixed vertical position in the mushy zone decreases and a larger volume of ice is produced, which increases the solute concentration of the solution trapped in the interstitial mushy space. As a result, the solid fractions in general grow with time. The agreement with the predictions by equation (15) is fair. The observed discrepancies may be due to properties of equation (15), whose accuracy deteriorates as the concentration increases. It is also probable that the equilibrium condition is not always achieved during the experiment, as it is seen in Figure 8.

Below we show some detailed results for the experimental condition No.2 ($C_0 = 5\text{wt\%},\ T_h = 0°\text{C},\ T_c = -8°\text{C}$) in Figures 7, 8 and 9. Figure 7 shows the time evolution of the vertical temperature distribution. Due to the relatively high solid fraction, conduction heat transfer dominates in the mushy layer, and this is in accord

with equation (14). On the other hand, convection heat transfer is a dominant mode in the liquid layer. The sharp temperature gradients in the top and the bottom boundary layers, and the uniform temperature in the middle are typical features of thermal convection heated from below.

The time evolution of the solute concentration is shown in Figure 8. The solute concentration increases linearly towards the top cooling plate in the mushy layer. Since the temperature also varies linearly in the mushy layer, the solid and the liquid phases appear in equilibrium. The concentration is almost constant throughout the liquid layer during the early times of the experiment. At this stage the assumption that the liquid layer is well mixed by vigorous thermal convection seems to be valid. However, as the time progresses, the accumulation of solute over the bottom plate is observed. The solute concentration near the bottom stabilizes the system, and as a result the thermal convection is obstructed. The solute concentrations and the temperatures measured in the mushy layer are plotted on the phase diagram as seen in Figure 9. The experimentally measured values are almost in accord with the liquidus line, implying that the mushy layer is in the equilibrium condition most of the time. This validates the basis on which equation (10) is formulated in order to compute the amount of solute in the mushy layer. Figure 10 shows a photo of the solid layer grown from above. Because of the many dendrites in the solid layer, it is non-transparent, and is thus different from the clear dense ice grown in pure water.

[Figure 5]

[Figure 6]

[Figure 7]

[Figure 8]

*[**Figure 9**]*

*[**Figure 10**]*

8. Natural convection in the Mushy Layer

Wettlaufer et al.[6] conducted research on ice formation from sea water, by cooling aqueous sodium-chlorite solution from above. They claimed that the ejection of solute-enriched residual to the liquid layer was a consequence of onset of compositional convection in the entire mushy region. The onset condition is governed by the concentration gradient, not by the temperature gradient. Therefore, the onset condition of convection is properly described by the salinity Rayleigh number,

$$Ra_{mC} = \frac{g\beta_C \Delta C K f}{\alpha_m \nu}. \tag{21}$$

where ΔC, K, α_m, β_C are the concentration difference between the top and bottom of the mushy zone, the permeability that is a function of the average solid fraction ϕ, the thermal diffusivity in the mushy zone, and the volume expansion coefficient by concentration respectively. When the compositional convection sets in, the solute ejection to the lower liquid layer increases measurably and the solid fraction in the mushy zone starts growing. Since Ra_{mC} in equation (21) is a fixed number at criticality,

$$\left(f\Delta C \right)^{-1} \propto K\left(\phi\right) \tag{22}$$

must hold. Wettlaufer et al.[6] obtained experimentally that at criticality $f\Delta C \simeq 30$ for $\phi \simeq 0.5$, and $f\Delta C \simeq 100$ for $\phi \simeq 0.8$ respectively. In the present experiment, the measurable solute increase in the liquid layer is observed in five hours after the cooling is initiated (see Figure 8). It is at this moment when the compositional convection

begins in the present experiment, and where the corresponding value takes $f\Delta C = 40 \sim 60$ over a range of a solid fraction $\phi = 0.6 \sim 0.8$. This agrees with Wettlaufer's results. However, it seems that the convection is not strong enough to distort the linear profile of the temperature in the mushy zone.

Next we will consider the possibility of thermal convection in the mushy zone. As seen in Figure 7, there is a maximum temperature difference of $7\,^{\circ}\mathrm{C}$ across the mushy layer, and therefore, the occurrence of thermal convection can not be immediately excluded. The mushy layer consists of many dendrites, the average solid fraction varies from 0.4 to 0.9, and the interstitial space is occupied by the enriched residual solution. In order to determine the criticality, the permeability of the mushy zone is needed, which can be calculated by Carman-Kozeny's equation[20, 21],

$$K = \frac{d^2 (1-\phi)^3}{180\phi^2}, \tag{23}$$

where d is the diameter of packed particle. The Rayleigh number based on the temperature difference between the two horizontal boundaries is given by

$$Ra_m = \frac{g\beta\Delta TKf}{\alpha_m \nu}. \tag{24}$$

The critical Rayleigh number of the onset of convection for an impermeable with constant temperature boundaries is known as $4\pi^2 \cong 40$ [20]. However, if the two horizontal boundaries are permeable, the critical Rayleigh number decreases to 12. In general the critical value becomes smaller, as the boundary conditions become less constrained. Therefore, in the present case, the critical value can be between 12 and 40. In order to evaluate the permeability of the mushy zone, we assume that the dendrite porous matrix can be replaced with packed particles, whose diameters are in a range of

d=0.1 and 0.3. Taking the maximum mushy layer thickness $f = 80\text{mm}$, and the minimum solid fraction $\phi = 0.2$ (corresponding to the largest void fraction), the Rayleigh number is always less than unity. Therefore, convection in the mushy zone due to the temperature differences is not likely in the present experiments.

9. Conclusions

In a rectangular box with the top boundary is kept at either $-6°\text{C}$ or $-8°\text{C}$, and the bottom boundary kept at $0°\text{C}$, aqueous sodium nitrite solution at either $5\text{wt\%}$ or $10\text{wt\%}$ is solidified from the top boundary. Under this condition the mushy layer consisting of a dendrite structure, starts growing from the cooling top boundary. Meanwhile the liquid layer in the vessel is generally well stirred by vigorous thermal convection, and the solute concentration is nearly uniform over the entire space, except for the region close to the bottom plate, where the solute concentration becomes slightly larger. Based on that we have obtained the following results:

(1) The time evolutions of the solid layer, the vertical temperature, and the solute concentration distributions in the vessel, are measured experimentally and the results are presented in graphical forms.

(2) Assuming that the vigorous convection is ensuing in the liquid layer, and that the convective heat flux is constant on the mushy layer front over the time interval to reach steady state, a one-dimensional analytical model has been developed to predict the time-evolution of the mushy layer and its space-averaged solid fraction. The analytical model predicts well the growth of the mushy layer thickness and the solid fraction.

(3) In the present experiment, it takes two to five hours before the compositional convection commences in the mushy layer, and the expelled solute starts descending to the liquid layer. As a consequence, the solute concentration in the liquid begins to increase, and the solid fraction ϕ in the mushy zone also starts to grow after this moment.

Literature Cited

1. Saito, T. Moving Boundary Heat Transfer. Youkendo; 1993 (in Japanese).
2. Ozoe, H. Czochralski Melt Convection Controlled by an External Magnetic Field. Journal of Japan Society of Fluid Mechanics, 2000; 19-5: 296-305 (in Japanese).
3. Tada, Y., Hayashi, Y. Heat transfer and Viability of Cell during freezing of Biological Tissue. Thermal Science and Engineering, 1998; 37-45: 13-20.
4. Hardee, H.C. Convective Heat Extraction from Molten Magma. J. Volcanol. Geotherm. Res., 1981; 10: 175-193.
5. Kimura, S. and Vynnycky, M. Time History of Ice-layer Formation at the Cooled Top Boundary and Its Dynamic Response to the Time-Varying Cooling Temperature. Moving Boundaries (edited by Saeler,B., Brebbia,C.A. and Power,H), WIT press; 1999: 47-56.
6. Wettaufer, J. S. et al. Natural convection during solidification of an alloy from above with application to the evolution of sea ice. J. Fluid Mech., 1997; 344: 291-316.
7. Nishimura, T., et al. Doublle-Diffusive Convection during Solidification of a Binary System. Transactions of the Japan Society of Mechanical Engineers, Series B, 1992; 58-548: 490-496 (in Japanese).
8. Copley, S.M. et al. The origin of freckles in binary alloys. Metall. Trans. A1, 1970; 2193-2204.
9. Chen,C.F., Chen, F. Experimental study of directional solidification of aqueous ammonium chloride solution. J.Fluid Mech., 1991; 227: 567-586.
10. Tait, S., Jaupart,.C. Compositional convection in a reactive crystalline mush and melt differentiation. J. Geophys. Res., 1992; 97: 6735-6756.

11. Chen,C.F., Turner, J.S. Crystallization in a Double-Diffusive System. J. Geophys. Res., 1980; 85-B5: 2573-2593.
12. Okada, M., Goto, K., Murakami, M. Solidification of an aqueous solution in a Rectangular cell with hot and cold vertical walls. Transactions of the Japan Society of Mechanical Engineers, Series B, 1990; 56-526: 1790-1795 (in Japanese).
13. Beckerman, C., Viskanta, R. Double-diffusive convection during dendritic solidification of a binary mixture. Physical Chemical Hydrodynamics, 1988;10-2: 195-213.
14. Thompson, M E., Szekely, J. Mathmatical and physical modelling of double diffusive convection of aqueous solutions crystallizing at a vertical wall. J.Fluid Mech., 1988;187: 409-433.
15. Huppert, H.E. The fluid mechanics of solidification. J. Fluid Mech., 1990; 212: 209-240.
16. Huppert, H. E., Worster, M.G.. Dynamic solidification of a binary melt. Nature, 1985; 314-25: 703-707.
17. Brewster, R.A., Gebhart, B. The effects of supercooling and freezing on natural convection in seawater. Int. J. Heat Mass Transfer, 1994; 37-4: 543-552.
18. Washburn, E.W.(ed.), International Critical Tables McGraw-Hill;1929.
19. Holman, J.P. Heat Transfer (Forth Edition), McGraw-Hill;1976).
20. Bejan, A. Convection Heat Transfer, John-Wiley; 1984.
21. Nield, D.A. and Bejan, A., Convection in Porous Media, 2nd edition, Springer-Verlag; 1998.

Figure and Table Captions

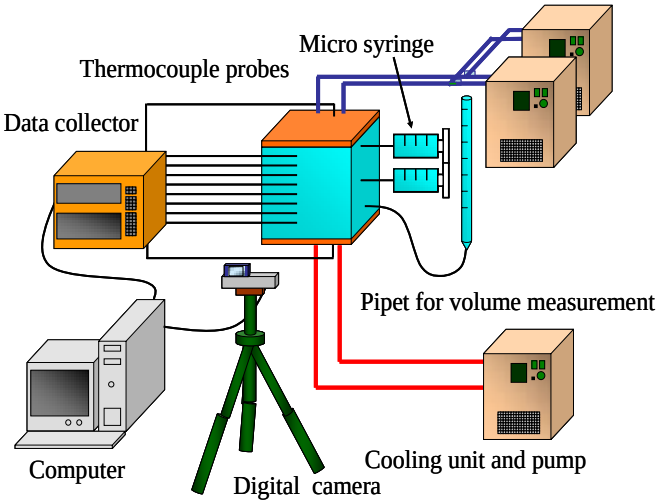

Fig. 1. Radiation reflection on real surface.

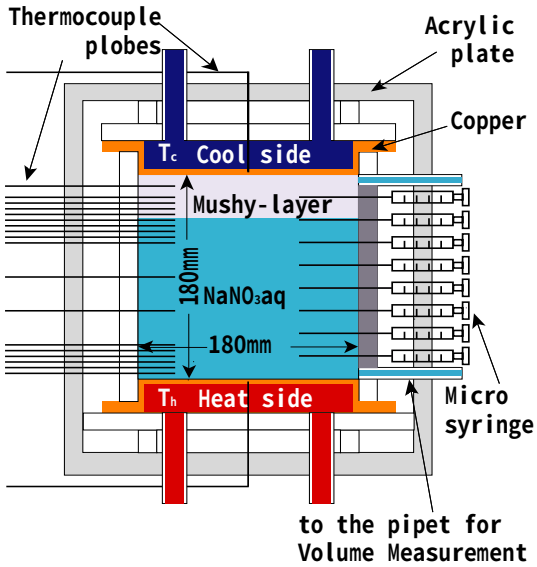

Fig. 4. Detailed sketch of experimental vessel

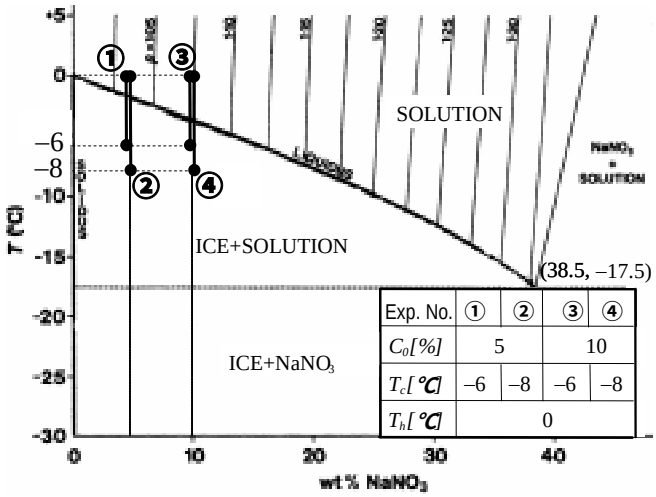

Fig.3 Phase equilibrium diagram

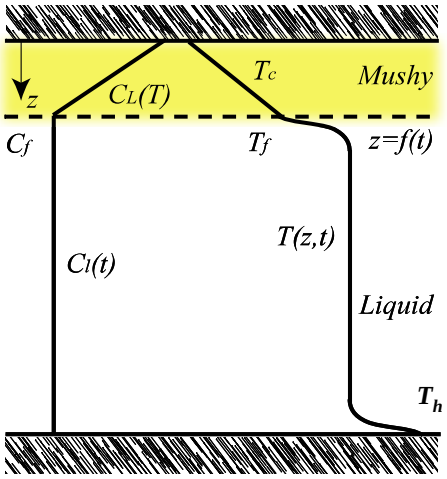

Fig. 4. Schematic of one-dimensional model

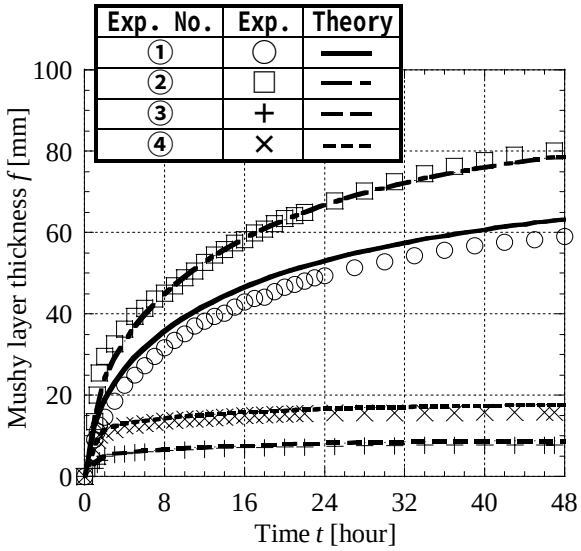

Fig.5 Growth of ice thickness with time

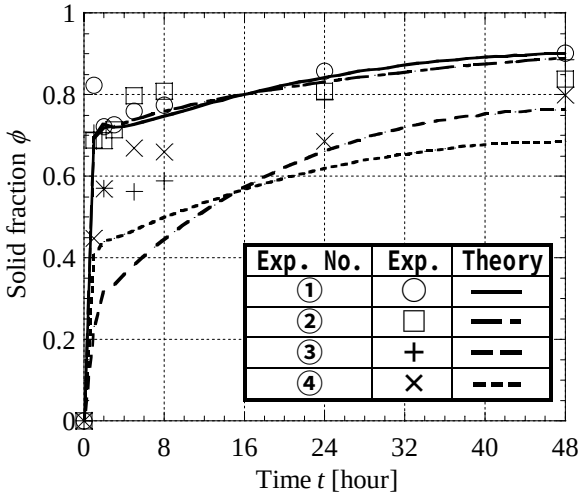

Fig.6 Growth of average solid fraction with time

Exp. No.②（C_0=5wt%, T_h=0°C, T_c=−8°C）

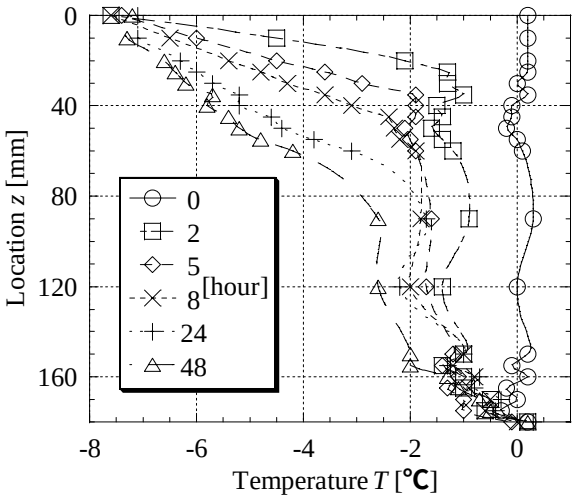

Fig.7 Vertical temperature evolution with time

Exp. No.②（C_0=5wt%, T_h=0°C, T_c=−8°C）

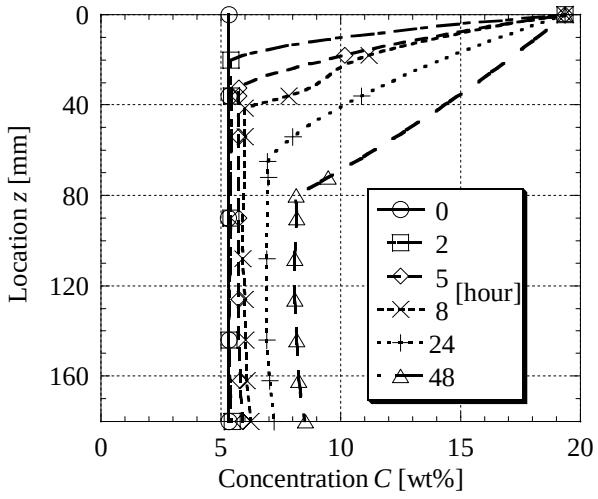

Fig.8 Vertical concentration evolution with time

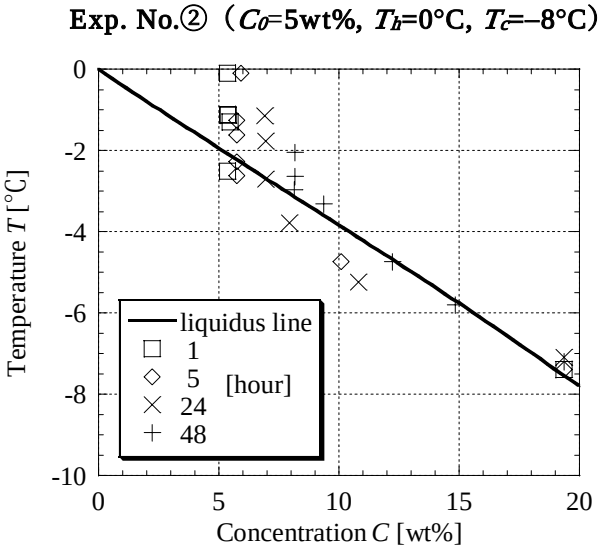

Fig.9 Measured temperature and concentration data on the phase diagram

Fig.10 Mushy layer grown from above

Table 1 Vertical heat transfer rate at steady state [W]

No.	①	②	③	④
Exp.	19.5	18.3	53.6	74.5
Eq.(18)	107.8	112.4	121.2	122.7